

Emission from Charge Recombination during the Pulse Radiolysis of Arylethynylpyrenes

Shingo Samori,[†] Sachiko Tojo,[†] Mamoru Fujitsuka,[†] Shu-Wen Yang,[‡] Tong-Ing Ho,[‡] Jye-Shane Yang,[‡] and Tetsuro Majima^{*,†}*Institute of Scientific and Industrial Research, Osaka University, Mihogaoka 8-1, Ibaraki, Osaka 567-0047, Japan, and Department of Chemistry, National Taiwan University, Taipei 10617, Taiwan**Received: April 1, 2006; In Final Form: May 4, 2006*

Emission from several 1-(arylethynyl)pyrenes with a substituent on the aryl group (REPy, R = phenyl (PEPy), 4-dimethylaminophenyl (NPEPy), 4-isopropoxyphenyl (OPEPy), 2-quinonyl (QEPy), and 9-(10-cyanoanthracenyl) (AEPy)) was studied with time-resolved fluorescence measurements during pulse radiolysis in benzene. NPEPy and AEPy showed only monomer emission, while PEPy, OPEPy, and QEPy showed both monomer and excimer emissions during pulse radiolysis. In addition, REPy's also showed long-lived emissions with very weak intensities in the absence of oxygen, which were assigned to the "P-type" delayed fluorescence derived from the triplet–triplet annihilation. The formation of REPy's in the singlet excited state (¹REPy*) can be interpreted as the charge recombination between the REPy radical cation and anion (REPy^{•+} and REPy^{•-}, respectively), which are initially generated from the radiolytic reaction in benzene. Both the highest occupied molecular orbital (HOMO) and the lowest unoccupied molecular orbital (LUMO) of PEPy are localized on the 1-pyrenyl (Py) moiety, while the HOMO of REPy's with an electron donating or withdrawing substituent on the benzene ring (R_DEPy such as NPEPy and OPEPy or R_AEPy such as QEPy and AEPy) is mainly localized on the donor moieties (R_D or Py) and the LUMO on the acceptor ones (Py or R_A, respectively). Therefore, it is suggested that the one-electron oxidation and reduction of REPy's can occur from the donor and acceptor moieties, respectively. This scheme reasonably explains the relationship between the annihilation enthalpy changes ($-\Delta H^\circ$) for the charge recombination of REPy^{•+} and REPy^{•-} and the singlet excitation energies (E'_{s_1}) of the REPy's. The results are compared with those in electrogenerated chemiluminescence.

Introduction

The detachment and attachment of an electron from and to a neutral solute molecule (M) generates radical cations (M^{•+}) and anions (M^{•-}), respectively, as important ionic intermediates in photochemistry, electrochemistry, and radiation chemistry.¹ When both M^{•+} and M^{•-} are generated in solution, the charge recombination between M^{•+} and M^{•-} occurs to form M in the singlet excited states (¹M*) emitting the light.² This process is significant because electrochemical energies can be converted to photochemical energies depending on M forming ¹M*. Much attention has been recently paid to electrogenerated chemiluminescence (ECL) of various types of M's, which originates from the charge recombination between M^{•+} and M^{•-} generated from the electrochemical oxidation and reduction on the electrodes, respectively.

In previous papers, we proposed the emission mechanisms of donor–acceptor-type M's with an ethynyl linkage (PE) such as donor-substituted phenylquinolinylethynes (PnQs),^{3a} phenyl-(9-acridinyl)ethynes (PADs), and phenyl(9-cyano-10-anthracenyl)ethynes (PANs),^{3b} which are known as ECL-active M's,⁴ during pulse radiolysis in benzene (Bz). On the basis of the transient absorption and emission measurements and steady-state measurements, the formation of donor–acceptor-type PEs in the singlet excited state (¹PE*) can be interpreted as the charge

recombination between PE^{•+} and PE^{•-}, which are generated initially from the radiolytic reaction in Bz. From the relationship between the annihilation enthalpy change ($-\Delta H^\circ$) in the charge recombination and the singlet excitation energy, it is suggested that the positive and negative charges are localized on the donor moiety of PE^{•+} and acceptor moiety of PE^{•-}, respectively.

In the electrochemical reaction of PE in CH₃CN, only excimer emission was observed.⁴ However, PnQ showed only monomer emission,^{3a} and PAD and PAN showed monomer and excimer emission during pulse radiolysis in Bz.^{3b} These results indicate that the emission mechanism during the pulse radiolysis of PE is different from that in the electrochemical reaction, although it is unclear why the two mechanisms are different.

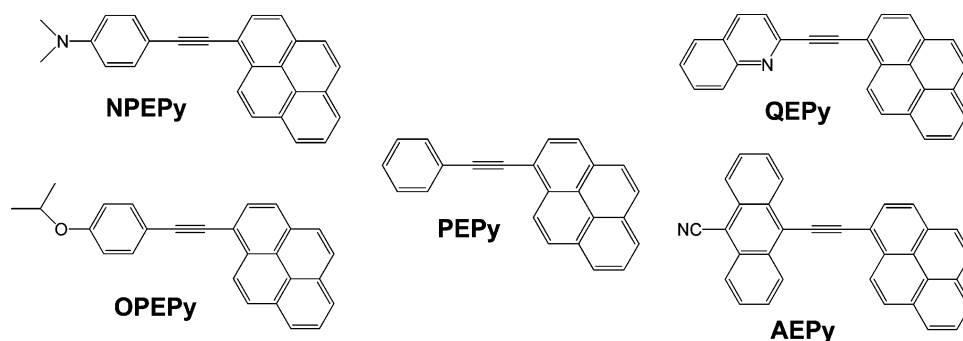
In this paper, we report the emission from the charge recombination between radical cations and radical anions of 1-phenylethynylpyrene (PEPy) and REPy, where R = 4-dimethylaminophenyl (NPEPy), 4-isopropoxyphenyl (OPEPy), 2-quinonyl (QEPy), and 9-(10-cyanoanthracenyl) (AEPy), with electron donating or withdrawing substituents on the benzene ring (R_DEPy such as NPEPy and OPEPy or R_AEPy such as QEPy and AEPy, the subscripts D and A denote donor and acceptor substituents, respectively) during pulse radiolysis in Bz. In addition, pyrene was also examined as the parent unsubstituted REPy. Through the use of the pulse radiolysis technique, both REPy^{•+} and REPy^{•-} can be generated at the same time in Bz. It is expected that ¹REPy*, ³REPy*, and/or ¹(REPy)₂* can be generated from the charge recombination between REPy^{•+} and REPy^{•-} during the pulse radiolysis of

* Author to whom correspondence should be addressed. Phone: +6-6879-8495. Fax: +6-6879-8499. E-mail: majima@sanken.osaka-u.ac.jp.

[†] Osaka University.

[‡] National Taiwan University.

CHART 1



REPy's in Bz, when REPy^{*+} and REPy^{*-} are produced at sufficient concentrations.

The fluorescence moieties for donor–acceptor-type PnQ, PAD, and PAN are the acceptor moieties quinoline, acridine, and 9-cyanoanthracene, respectively. Therefore, it is expected that the emission results from the 1-pyrenyl (Py) moieties with electron donor and/or acceptor characteristics during the pulse radiolysis of REPy's. The presence or absence of excimer emission may depend on the electronic properties of the REPy's. The emission mechanisms of the ECL-active REPy's during pulse radiolysis are discussed based on the time-resolved transient absorption and emission measurements, providing valuable insights for molecular design with efficient luminescence characteristics.

Experimental Section

Steady-State Measurements. UV spectra were recorded in Bz with a Shimadzu UV-3100PC UV–vis spectrometer using a transparent rectangular cell made from quartz ($1.0 \times 1.0 \times 4.0 \text{ cm}^3$, path length of 1.0 cm). Fluorescence spectra were measured by a Hitachi 850 spectrofluorometer.

Pulse Radiolysis. Pulse radiolysis experiments were performed using an electron pulse (28 MeV, 8 ns, 0.87 kGy per pulse) from a linear accelerator at Osaka University. Except for AEPy, all the sample solutions were prepared at a 5 mM concentration in Bz in a rectangular quartz cell ($0.5 \times 1.0 \times 4.0 \text{ cm}^3$, path length of 1.0 cm). Because the solution of 5 mM AEPy was not prepared in Bz due to its poor solubility, it was prepared in saturated concentrations. These solutions were saturated with Ar gas by bubbling with it for 10 min at room temperature before irradiation. The kinetic measurements were performed using a nanosecond photoreaction analyzer system (Unisoku, TSP-1000). The monitor light was obtained from a pulsed 450 W Xe arc lamp (Ushio, UXL-451-0), which was operated by a large current pulsed-power supply that was synchronized with the electron pulse. The monitor light was passed through an iris with a diameter of 0.2 cm and sent into the sample solution perpendicular to the electron pulse. The monitor light passing through the sample was focused on the entrance slit of a monochromator (Unisoku, MD200) and detected with a photomultiplier tube (Hamamatsu Photonics, R2949). The transient absorption and emission spectra were measured using a photodiode array (Hamamatsu Photonics, S3904-1024F) with a gated image intensifier (Hamamatsu Photonics, C2925-01) as a detector. To avoid pyrolysis of the sample solution by monitor light, a suitable cutoff filter was used.

Fluorescence Lifetime Measurements. Fluorescence lifetimes were measured by the single photon counting method using a streakscope (Hamamatsu Photonics, C4334-01) equipped

TABLE 1: Photophysical Properties of the REPy's and Pyrene in CH_3CN , Hexane, and Bz

compound	in CH_3CN			in hexane		in Bz			
	$\lambda_{\text{max}}^{\text{Abs}}$ (nm)	$\lambda_{\text{max}}^{\text{Fl}}$ (nm)	τ_{fl} (ns)	$\lambda_{\text{max}}^{\text{Abs}}$ (nm)	$\lambda_{\text{max}}^{\text{Fl}}$ (nm)	$\lambda_{\text{max}}^{\text{Abs}}$ (nm)	$\lambda_{\text{max}}^{\text{Fl}}$ (nm)	ϕ_{fl}	τ_{fl} (ns)
NPEPy	388 ^a	540 ^a	3.47 ^a	405 ^a	421 ^a	390	456	0.62	1.88
OPEPy	386 ^a	480 ^a	1.98 ^a	386 ^a	395 ^a	376	404	0.97	1.84
PEPy	381 ^a	392 ^a	4.85 ^a	382 ^a	389 ^a	386	395	0.85	3.50
QEPy	395 ^a	444 ^a	2.05 ^a	397 ^a	402 ^a	404	423	0.86	1.96
AEPy	472 ^a	556 ^a	4.60 ^a	472 ^a	482 ^a	481	509	0.41	3.27
pyrene	335	393	340 ^b	333	385	338	394	0.77 ^b	311 ^b

^a Reference 5. ^b Reference 6.

with a polychromator (Acton Research, SpectraPro150). An ultrashort laser pulse was generated with a Ti:sapphire laser (Spectra-Physics, Tsunami 3941-M1BB, full width at half-maximum of 100 fs) pumped with a diode-pumped solid-state laser (Spectra-Physics, Millennia VIIIIs). For the excitation of samples, the output of the Ti:sapphire laser was converted to the third harmonic oscillation with a harmonic generator (Spectra-Physics, GWU-23FL).

Results and Discussion

Chart 1 depicts the chemical structures of five REPy's. NPEPy and OPEPy have a phenylethynyl group with strong and weak electron donor substituents, respectively. However, QEPy and AEPy have an aryl ethynyl group with strong and weak electron withdrawing characteristics, respectively. In addition to R_D REPy and R_A AEPy, PEPy was studied to elucidate the effects of the substituents.⁵

Photophysical and Electrochemical Properties. The photophysical properties of the REPy's and pyrene in CH_3CN ($\epsilon = 37.5$), hexane ($\epsilon = 1.89$), and Bz ($\epsilon = 2.28$) are listed in Table 1. The ground-state absorption peaks of the REPy's in these solvents had little influence on the solvent polarity. However, the fluorescence peaks of the REPy's in CH_3CN or Bz except for PEPy were observed at longer wavelengths than those in hexane due to the solvent polarity (Figure 1). PEPy has been found to have no intermolecular charge transfer (ICT) character in the excited state because only a slight red shift was observed in CH_3CN .⁵ However, strong ICT is reasonably suggested for NPEPy and AEPy with strong electron donating and withdrawing substituents, respectively. Both OPEPy and QEPy with weak electron donating and withdrawing substituents, respectively, indicated weak ICT in CH_3CN . In Bz, donor–acceptor-type REPy's showed a red shift in the emission maxima. It was shown that a high fluorescence quantum yield (ϕ_{fl}) was observed for PEPy (0.85) and that the lowest ϕ_{fl} value (0.41) was for AEPy in Bz. Although the fluorescence lifetimes (τ_{fl}) of REPy's in Bz were slightly shorter than those in CH_3CN ,⁵ the dependence of τ_{fl} on the REPy was similar in Bz and

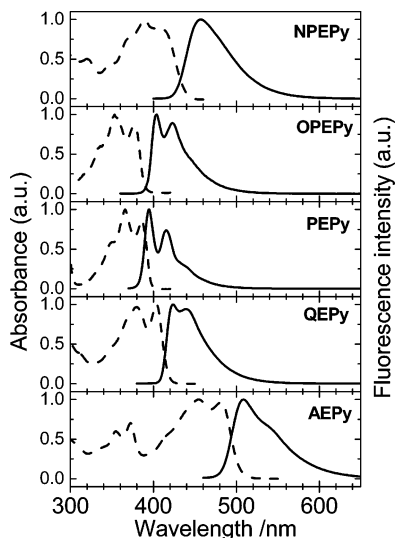


Figure 1. Absorption (broken line) and fluorescence (solid line) spectra obtained by the steady-state absorption and fluorescence measurement of REPy's in Ar-saturated Bz (10^{-5} M).

TABLE 2: Electrochemical Properties of the REPy's in CH_3CN and Pyrene in 1:1 $\text{CH}_3\text{CN}/\text{Bz}$

compound	concentration (mM)	in CH_3CN			$\lambda_{\text{max}}^{\text{ECL}}$	
		E_{ox} (V)	E_{red} (V)	$-\Delta H^\circ$ (eV)	(nm)	(eV)
NPEPy	1.0 ^{a,b}	0.92 ^b	-0.92 ^b	1.68 ^b	510 ^b	2.431 ^b
OPEPy	0.5 ^{a,b}	1.33 ^b	-0.90 ^b	2.07 ^b	509 ^b	2.436 ^b
PEPy	1.0 ^{a,b}	1.41 ^b	-0.92 ^b	2.17 ^c	<i>c</i>	<i>c</i>
QEPy	0.5 ^{a,b}	1.18 ^b	-1.11 ^b	2.13 ^c	<i>c</i>	<i>c</i>
AEPy	saturated ^{a,b}	0.91 ^b	-0.83 ^b	1.58 ^b	<i>c</i>	<i>c</i>
pyrene	1.0 ^e	1.07 ^d	-2.38 ^d	3.29	513, 644 ^e	2.417

^a Different concentrations were chosen due to varying solubility for each compound. ^b Reference 5. ^c No ECL was observed. ^d Reference 9. Potential was estimated vs Ag/Ag^+ . ^e Reference 7.

CH_3CN . These results suggest that the excited-state properties of REPy's in Bz and CH_3CN are similar but different from those in hexane. Therefore, ICT is also assumed for donor-acceptor-type REPy's in Bz but not in hexane.

The electrochemical properties of REPy's in CH_3CN are listed in Table 2. Through the use of a setup consisting of a fluorescence spectrophotometer and voltammograph with a PC interface, ECL emissions of NPEPy (1.0 mM) and OPEPy (0.5 mM) were observed with peaks at 510 and 509 nm in CH_3CN , respectively, in the presence of 0.05 M tetrabutylammonium perchlorate (TBAP) as the supporting electrolyte.⁵ The ECL emission for NPEPy was assumed to be derived from the H-type excimer, while the usual π -stacked excimer ECL emission was observed in the ECL for OPEPy. However, REPy's without a donor moiety and with electron acceptor moieties do not emit ECL emissions. It has been reported that pyrene emitted a very weak excimer ECL emission at 513 nm together with a weak emission at 644 nm that is assigned to reaction products of pyrene^{•+}.⁷ To elucidate the ECL emission mechanism, the annihilation enthalpy change ($-\Delta H^\circ$) for the charge recombination between $\text{M}^{\bullet+}$ and $\text{M}^{\bullet-}$ is calculated by eq 1⁸

$$-\Delta H^\circ = [(E_{\text{ox}} - E_{\text{red}})]^{\epsilon_s} - \Delta G_{\text{sol}}^{\epsilon_s} - w_{a,\mu} + T\Delta S^\circ \quad (1)$$

where E_{ox} and E_{red} are the oxidation and reduction potentials of M, respectively, and ϵ_s , ΔG_{sol} , and $w_{a,\mu}$ represent the static dielectric constant of the solvent, the free energy of solvation, and the work required to bring $\text{M}^{\bullet+}$ and $\text{M}^{\bullet-}$ within a likely

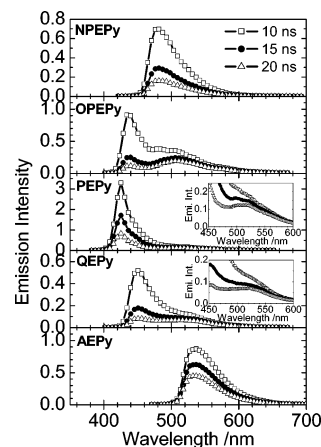


Figure 2. Emission spectra recorded at time $t = 10$ (open square), 15 (solid circle), and 20 (open triangle) ns after an electron pulse during the pulse radiolysis of the REPy's in Ar-saturated Bz. Inset: Expanded spectra in the longer wavelength region.

separation distance, respectively. In CH_3CN , $-\Delta H^\circ$ can be expressed using E_{ox} and E_{red} measured in CH_3CN by eq 2^{4,5}

$$-\Delta H^\circ = E_{\text{ox}} - E_{\text{red}} - 0.16 \text{ eV} \quad (2)$$

The calculated $-\Delta H^\circ$ values for the REPy's are listed in Table 2. $-\Delta H^\circ$ values for NPEPy and OPEPy are not sufficiently larger than the ECL maximal energies, and hence, $^3\text{REPy}^*$ is generated and followed by triplet-triplet annihilation, giving $^1\text{REPy}^*$, which corresponds to the ECL (T-route).

Emission Spectra Observed during the Pulse Radiolysis of REPy's in Bz. The time-resolved emission spectra were observed to show a monotonic decay after an electron pulse during the pulse radiolysis of REPy's in Ar-saturated Bz (Figure 2). All REPy's showed an emission maximum at 423–523 nm after an electron pulse during pulse radiolysis. For PEPy, OPEPy with a weak electron donor substituent, and QEPy with a weak electron withdrawing substituent, another emission maximum, assigned to be excimer emission, was observed at a longer wavelength during pulse radiolysis (Figure 2, inset), although they were not observed in the steady-state fluorescence measurement even at a high concentration (5 mM).^{3b} Because the fluorescence maxima of $\text{R}_\text{D}\text{EPy}$ and $\text{R}_\text{A}\text{EPy}$ were observed at longer wavelengths than that of PEPy, an emissive ICT is assumed for $\text{R}_\text{D}\text{EPy}$ and $\text{R}_\text{A}\text{EPy}$ during pulse radiolysis in Bz. In addition, the shapes of the emission spectra of PEPy, OPEPy, and QEPy were different from those observed in the steady-state measurement, and emission maxima observed at the shorter wavelength region disappeared because of the self-absorption as a result of the high concentrations of the REPy's. The monomer and excimer emissions were also observed during the pulse radiolysis of pyrene in Bz. For pyrene, the formation of excimer emission was clearly observed in the steady-state measurement at a high concentration (5 mM). The radiolysis-induced emission intensities of the REPy's and pyrene were determined from the total amount of emission and are summarized in Table 3. It is assumed that the emissions of the REPy's mainly correspond to the Py moiety, which is known as an excellent fluorophore.

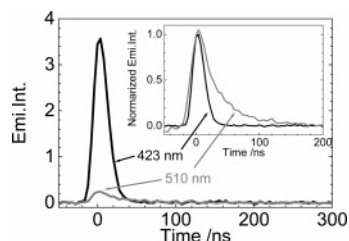
In the electrochemical reaction, only two compounds (NPEPy and OPEPy) emit an ECL emission.⁵ However, all REPy's showed fluorescence during pulse radiolysis in Bz. These results indicate that the emission mechanism during the pulse radiolysis of REPy's is different from that in the electrochemical reaction. It was found that the emission intensity of PEPy (100) was the

TABLE 3: Emission Maxima (λ_{Em}) and Radiolysis-Induced Emission Intensities of the REPy's and Pyrene Observed after an Electron Pulse during Pulse Radiolysis in Ar- and Air-Saturated Bz

compound	λ_{Em} (nm)	radiolysis-induced emission intensity ^a (%)	
		in Ar-saturated Bz	in air-saturated Bz
NPEPy	478	57.7	36.7
OPEPy	437, 508	65.8	42.1
PEPy	423, 510	100	54.7
QEPy	450, 523	66.9	43.9
AEPy	530	17.6 (saturated) ^b	9.01 (saturated) ^b
pyrene	393, 475	68.6	8.53

^a Relative to the emission intensity for PEPy in Ar-saturated Bz. Emission intensity was determined from the total amount of emission.

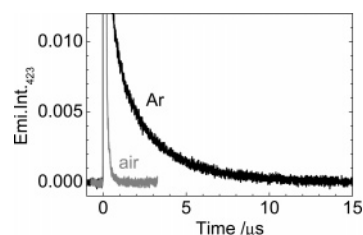
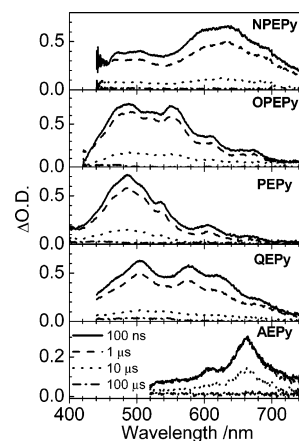
^b Saturated concentration due to poor solubility.

**Figure 3.** Time profiles of the emissions observed during the pulse radiolysis of PEPy in Ar-saturated Bz (5 mM) at 423 and 510 nm. Inset: Emission intensities were normalized to be 1.0.

highest and that of pyrene (68.6) was higher than those of donor–acceptor-type REPy's (17.6–66.9) in Ar-saturated Bz. However, only very weak emission was observed during the pulse radiolysis of quinoline^{3a} and diphenylacetylene,^{3b} which are the moieties of the parent unsubstituted REPy's in Bz. When the emission spectra of the REPy's and pyrene were measured in air-saturated Bz, the emission intensities decreased significantly. For pyrene, it significantly decreased (68.6 → 8.53).

Figure 3 shows time profiles of emissions observed at 423 (monomer emission) and 510 nm (excimer emission) of PEPy. In the inset of Figure 3, both initial emission intensities were normalized to be 1.0. It is suggested that the monomer and excimer were formed from the same precursor through the same reaction mechanism. OPEPy and QEPy also showed the same emission behavior. However, the excimer emission observed during the pulse radiolysis of pyrene in Bz formed with the decay of the monomer emission.

It was found that the emission time profiles observed during the pulse radiolysis of REPy's and pyrene in Ar-saturated Bz showed two components, short-lived with a high emission intensity and long-lived with a very low one. Even at a few microseconds after an electron pulse, the long-lived emission was observed to be assigned to delayed fluorescence derived from triplet–triplet annihilation (T-route). The time profiles of emission observed at 423 nm during the pulse radiolysis of REPy's in air-saturated Bz (in the presence of dissolved oxygen) showed no long-lived emission component as shown in Figure 4. It is clearly shown that the long-lived emission component was quenched by oxygen. The same quenching behavior was also observed at 510 nm. The quenching was observed for all compounds, indicating that the “P-type” delayed fluorescence¹⁰ was confirmed for REPy's and pyrene in Bz during pulse radiolysis. The P-type delayed fluorescence reflects on the transient behavior of REPy's and pyrene in the triplet excited state. In the presence of oxygen, the significant decrease of the emission intensity observed for pyrene shows that the emission for pyrene corresponds mainly to the P-type delayed fluorescence.

**Figure 4.** Time profiles of the transient emission intensities at 423 nm observed during the pulse radiolysis of PEPy in Ar- and air-saturated Bz (5 mM).**Figure 5.** Time-resolved transient absorption spectra observed at time $t = 100$ ns, 1, 10, and $100 \mu\text{s}$ after an electron pulse during the pulse radiolysis of the REPy's in Ar-saturated Bz. The sample solutions were prepared at a 5 mM concentration except for AEPy (saturated concentration due to poor solubility).

In the ECL experiment, the H-type excimer was assumed for NPEPy, while the usual π -stacked excimer was assumed for OPEPy. No emission for PEPy and R_AEPy was observed in the ECL. However, the monomer emission was observed for all PEPy's together with the excimer emission only for PEPy, OPEPy, and QEPy during pulse radiolysis in Bz. Because REPy^{•+} and REPy^{•-} are generated as the initial species during both pulse radiolysis and electrochemical reaction, the different emissive species may be attributed to the different experimental conditions such as solvent and concentrations of REPy, REPy^{•+}, and REPy^{•-}. The formation of ¹(R_DEPy)₂^{*} is preferred in acetonitrile, because of stabilization in a polar solvent, and at higher concentrations of R_DEPy, R_DEPy^{•+}, and R_DEPy^{•-} during the electrochemical reaction. However, the formation of ¹(PEPy)₂^{*}, ¹(OPEPy)₂^{*}, and ¹(QEPy)₂^{*} is preferable in benzene because of the stabilization in a nonpolar solvent during pulse radiolysis.

Transient Absorption Spectra Observed during the Pulse Radiolysis of REPy's. Figure 5 shows the transient absorption spectra observed during the pulse radiolysis of REPy's in Ar-saturated Bz, which can be assigned to REPy^{•+}, REPy^{•-}, and/or ³REPy*. For donor–acceptor-type REPy's, the absorption bands at around 400–500 nm were not measured due to the strong ground-state absorption. In air-saturated Bz, the transient absorption observed at 486 nm decayed in the time scale of 10 μs during the pulse radiolysis of PEPy (Figure 6). To identify the transient species in detail, the transient absorption spectra of REPy's in Bz were measured during the 355-nm 5-ns laser flash photolysis (Supporting Information, Figure S1).³ The observed spectra with the band at 500 nm are quenched by oxygen and assigned to ³REPy*. Therefore, the transient absorption spectra, observed during the pulse radiolysis of REPy's in Ar-saturated Bz, are assigned mainly to ³REPy*.

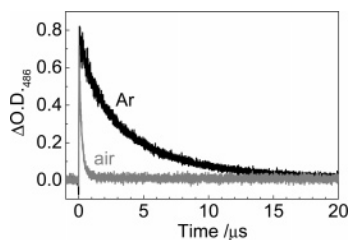


Figure 6. Time profiles of the transient absorption at 486 nm observed during the pulse radiolysis of PEPy (5 mM) in Ar- and air-saturated Bz.

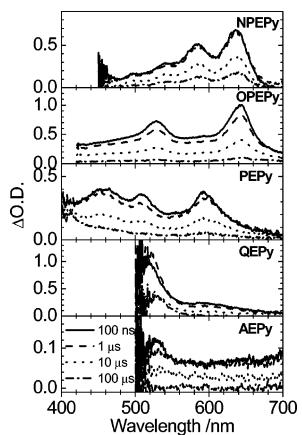


Figure 7. Time-resolved transient absorption spectra observed at time $t = 100$ ns, 1, 10, and $100 \mu\text{s}$ after an electron pulse during the pulse radiolysis of the REPy's in Ar-saturated DCE. The sample solutions were prepared at a 5 mM concentration except for AEPy (saturated concentration due to poor solubility).

To confirm the transient absorption spectra of $\text{REPy}^{+\bullet}$ and $\text{REPy}^{\bullet-}$, the pulse radiolysis of REPy's in Ar-saturated dichloroethane (DCE) and dimethylformamide (DMF) was also examined. It is established that $\text{M}^{+\bullet}$ is generated during the pulse radiolysis of M in DCE,^{3,11} while $\text{M}^{\bullet-}$ is generated in DMF.^{3,12} Figure 7 shows the transient absorption spectra observed during the pulse radiolysis of REPy's in Ar-saturated DCE. The absorption bands observed for all REPy's with a half-lifetime on the order of microseconds can be assigned to $\text{REPy}^{+\bullet}$. For $\text{QEPy}^{+\bullet}$, the absorption band was observed at around 520 nm and persisted even on a time scale longer than $100 \mu\text{s}$. It seems that Cl^- reacts with $\text{QEPy}^{+\bullet}$ to give a product having an absorption peak at approximately 520 nm. It should be noted that all $\text{REPy}^{+\bullet}$ showed the individual spectral shapes. For $\text{NEPy}^{+\bullet}$ and $\text{OPEPy}^{+\bullet}$, it is clearly shown that the strongest absorption peak was observed at approximately 640 nm. These absorption bands seem to correspond to phenylacetylene because phenylacetylene^{+\bullet} has been reported to have an absorption band at 622 nm.¹³ $\text{NEPy}^{+\bullet}$ and $\text{OPEPy}^{+\bullet}$ showed additional absorption peaks at 583 and 529 nm, respectively, suggesting the different electronic properties of $\text{NEPy}^{+\bullet}$ and $\text{OPEPy}^{+\bullet}$ from those of phenylacetylene^{+\bullet}, because of the substituents on the phenyl ring of $\text{NEPy}^{+\bullet}$ and $\text{OPEPy}^{+\bullet}$.

For $\text{PEPy}^{+\bullet}$, $\text{QEPy}^{+\bullet}$, and $\text{AEPy}^{+\bullet}$, absorption bands were observed mainly at approximately 500 nm. Pyrene^{+\bullet} has been reported to have a strong absorption at 450 nm with a broad absorption band at 400–800 nm.¹³ Therefore, the absorption bands for $\text{PEPy}^{+\bullet}$, $\text{QEPy}^{+\bullet}$, and $\text{AEPy}^{+\bullet}$, observed at longer wavelengths than those for pyrene^{+\bullet}, correspond to ethynyl-substituted pyrene^{+\bullet}. It has been reported that radical cations having an ethynyl group such as phenylacetylene^{+\bullet} and diphenylacetylene^{+\bullet} show an absorption band at 620–800 nm.¹³ It is assumed that the absorption band of ethynyl-substituted

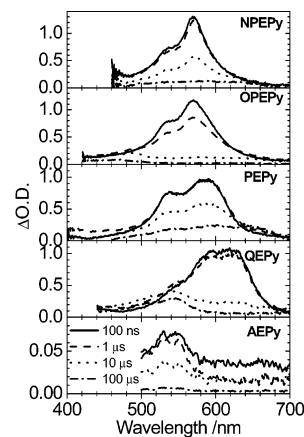


Figure 8. Time-resolved transient absorption spectra observed at time $t = 100$ ns, 1, 10, and $100 \mu\text{s}$ after an electron pulse during the pulse radiolysis of the REPy's in Ar-saturated DMF. The sample solutions were prepared at a 5 mM concentration except for AEPy (saturated concentration due to poor solubility).

pyrene^{+\bullet} shifted to the longer wavelength because of an ethynyl group. Thus, it seems that the spectral shapes of $\text{REPy}^{+\bullet}$ reflect the localized positive charges on $\text{REPy}^{+\bullet}$.

Figure 8 shows the transient absorption observed during the pulse radiolysis of REPy in Ar-saturated DMF. The absorption bands observed for all REPy's with a half-lifetime on the order of microseconds can be assigned to $\text{REPy}^{\bullet-}$. For $\text{PEPy}^{\bullet-}$ and $\text{QEPy}^{\bullet-}$, the broad absorption band was observed at 610 and 520 nm, respectively, and persisted even on a time scale longer than $100 \mu\text{s}$. It seems that $\text{PEPy}^{\bullet-}$ or $\text{QEPy}^{\bullet-}$ reacts to give a product having an absorption peak at 610 or 520 nm, respectively. The absorption spectra for $\text{PEPy}^{\bullet-}$, $\text{NEPy}^{\bullet-}$, and $\text{OPEPy}^{\bullet-}$ showed a band at approximately 520–620 nm with a shoulder at 530 nm and were almost equivalent with those observed at 100 ns after the electron pulse. The absorption peaks of $\text{QEPy}^{\bullet-}$ and $\text{AEPy}^{\bullet-}$ were observed at longer and shorter wavelengths, respectively, than that of $\text{PEPy}^{\bullet-}$. Since pyrene^{-\bullet} has been reported to have an absorption peak at approximately 500 nm,¹³ the absorption bands for $\text{NPEPy}^{\bullet-}$, $\text{OPEPy}^{\bullet-}$, and $\text{PEPy}^{\bullet-}$ were observed at longer wavelengths than that of pyrene^{-\bullet} to be assigned to ethynyl-substituted pyrene^{-\bullet}. In addition, phenylacetylene^{-\bullet} has absorption maxima at approximately 374 and 533 nm,¹³ quinoline^{-\bullet} has two absorption bands at 340–450 and 600–800 nm,¹³ and 9-cyanoanthracene^{-\bullet} has an absorption band at 500–700 nm.¹³ For $\text{QEPy}^{\bullet-}$, the transient absorption band was observed at 550–680 nm and assigned to ethynyl-substituted quinoline^{-\bullet}. For $\text{AEPy}^{\bullet-}$, the transient absorption band seems to be assigned to ethynyl-substituted 9-cyanoanthracene^{-\bullet}. Therefore, it is suggested that the spectral shapes of $\text{REPy}^{\bullet-}$ also reflect the localized negative charges on the Py moiety.

No or little emission was observed during the pulse radiolysis of REPy's in DCE or DMF, suggesting only $\text{REPy}^{+\bullet}$ or $\text{REPy}^{\bullet-}$ do not emit light. In other words, both $\text{REPy}^{+\bullet}$ and $\text{REPy}^{\bullet-}$ must be formed at the same time to observe the emission. In Bz, however, no transient absorption bands of $\text{REPy}^{+\bullet}$ and $\text{REPy}^{\bullet-}$ were observed immediately after an 8-ns electron pulse. Therefore, it is assumed that $\text{REPy}^{+\bullet}$ and $\text{REPy}^{\bullet-}$ immediately recombine to give $^1\text{REPy}^*$, $^3\text{REPy}^*$, and $^1(\text{REPy})_2^*$ (for PEPy, OPEPy, and QEPy) within a pulse duration.³ The transient absorption spectral data obtained during pulse radiolysis in Ar-saturated Bz, DCE, and DMF are summarized in Table 4.

Emission Mechanism. In Bz, $-\Delta H^\circ$ can be expressed by eq 3

TABLE 4: Transient Absorption Maxima (λ^{TA}) Observed during the Pulse Radiolysis of the REPy's in Ar-Saturated Bz, DCE, and DMF

compound	λ^{TA} (nm)		
	in Bz	in DCE	in DMF
NPEPy	505, 633	583, 638	535, 569
OPEPy	488, 552	529, 645	534, 570
PEPy	486, 535, 606	453, 508, 590	537, 587
QEPy	503, 577, 617	522, 587	619
AEPy	610, 663	531, 711	530

$$-\Delta H^\circ = E_{\text{ox}} - E_{\text{red}} + 0.29 \text{ eV} \quad (3)$$

$-\Delta H^\circ$ values for REPy's in Bz are shown in Table 5 with the emission maximal energies (E'_{S_1}) during pulse radiolysis.

Table 5 shows that $-\Delta H^\circ$ values for REPy's are smaller than E'_{S_1} , while that for pyrene is larger. The energy available in the charge recombination was sufficient to populate the S_1 state for pyrene, while those for REPy's were insufficient. If E_{T_1} of the REPy were smaller than $-\Delta H^\circ$, then it may be possible to populate the S_1 state via the T-route. In this case, the emission via the T-route was assumed to be observed as a delayed fluorescence and was clearly confirmed as shown in Figure 4. The relation between $-\Delta H^\circ$ and E'_{S_1} can explain the short-lived emission component observed for pyrene resulting from ${}^1\text{pyrene}^*$, which was formed through the direct charge recombination between $\text{pyrene}^{\bullet+}$ and $\text{pyrene}^{\bullet-}$ (S-route). Excimer emission was also observed in the case of pyrene, indicating the association of ${}^1\text{pyrene}^*$ with pyrene. However, the short-lived emission component observed for REPy's cannot be explained by the relation between $-\Delta H^\circ$ and E'_{S_1} , and the reaction process to form ${}^1(\text{REPy})_2^*$ is different from that for ${}^1\text{pyrene}_2^*$.

The highest occupied molecular orbital (HOMO) and the lowest unoccupied molecular orbital (LUMO) surfaces of REPy's in the ground state were calculated from density functional theory (DFT) calculations, indicating that both the HOMO and the LUMO of PEPy localize on the Py moiety.⁵ The one-electron oxidation can reflect on the character of the HOMO, while the one-electron reduction reflects on that of the LUMO. Thus, it is suggested that both oxidation and reduction of PEPy occur on the Py moiety. E_{ox} and E_{red} values of pyrene are 1.07 and -2.38 V (vs Ag/Ag^+).⁸ Therefore, the $-\Delta H^\circ$ value for the charge recombination between $\text{PEPy}^{\bullet+}$ and $\text{PEPy}^{\bullet-}$ can be estimated to be 3.74 eV from E_{ox} and E_{red} values of pyrene. Thus, $-\Delta H^\circ$ values are sufficiently larger than the E'_{S_1} values (2.93 eV).

The transient absorption spectral shapes of $\text{PEPy}^{\bullet+}$ and $\text{PEPy}^{\bullet-}$ (Figures 7 and 8) showed that both positive and negative charges are localized on the ethynyl-substituted Py moiety.

TABLE 5: Annihilation Enthalpy Changes ($-\Delta H^\circ$) and Emission Maximal Energies (E'_{S_1}) during the Pulse Radiolysis of the REPy's in Bz

compound	$-\Delta H^\circ$ (eV)	E'_{S_1} ^a (eV)
NPEPy	2.13	2.59
OPEPy	2.52	2.67
PEPy	2.62	2.93
QEPy	2.58	2.76
AEPy	2.03	2.34
pyrene	3.74	3.16

^a Estimated from the peak wavelength of the emission spectra observed during the pulse radiolysis.

Therefore, it is suggested that the charge recombination between $\text{PEPy}^{\bullet+}$ and $\text{PEPy}^{\bullet-}$ with localized charges on the Py moieties occurs to give ${}^1\text{PEPy}^*$ and ${}^1(\text{PEPy})_2^*$ during the pulse radiolysis of PEPy in Bz. In addition to those, the delayed fluorescence also occurs due to the formation of ${}^3\text{PEPy}^*$ (Scheme 1).

For donor-acceptor-type REPy's ($\text{R}_\text{D}\text{EPy}$ and $\text{R}_\text{A}\text{EPy}$), the HOMO is mainly localized on the donor moieties, and the LUMO is localized on the acceptor moieties.⁵ Therefore, it is suggested that the one-electron oxidation can occur from donor moieties, and the one-electron reduction on the acceptor moieties of the molecules. This scheme reasonably explains the emission mechanism during the pulse radiolysis of REPy's in Bz. For NPEPy, the $-\Delta H^\circ$ value of the donor moiety (corresponding to *N,N*-dimethylaniline) is 0.55 V ,^{10a} while that of the acceptor moiety (Py) is -2.38 V . Therefore, the $-\Delta H^\circ$ value for the charge recombination between $\text{NPEPy}^{\bullet+}$ and $\text{NPEPy}^{\bullet-}$ can be estimated to be 3.22 eV , which is sufficiently larger than the E'_{S_1} value. Similarly, the $-\Delta H^\circ$ values for QEPy and AEPy are larger than the E'_{S_1} values (Table 6).

The transient absorption spectral shapes of $\text{NPEPy}^{\bullet+}$ and $\text{OPEPy}^{\bullet+}$ (Figure 7) show that the positive charge is localized on ethynyl-substituted donor moieties (*N,N*-dimethylaniline and isopropoxybenzene, respectively) ($(\text{R}_\text{D}\text{E})^{\bullet+}\text{Py}$). For QEPy^{•+} and AEPy^{•+}, it is suggested that the positive charge is localized on the ethynyl-substituted Py moiety ($\text{Q}(\text{EPy})^{\bullet+}$). However, the transient absorption spectral shapes of $\text{REPy}^{\bullet-}$ show that the negative charge is localized on the ethynyl-substituted Py moiety ($\text{R}_\text{D}(\text{EPy})^{\bullet-}$) for $\text{R}_\text{D}\text{EPy}^{\bullet-}$ and the ethynyl-substituted acceptor moieties (quinoline and 9-cyanoanthracene) ($(\text{R}_\text{A}\text{E})^{\bullet-}\text{Py}$) for $\text{R}_\text{A}\text{EPy}^{\bullet-}$. Thus, the emissive ICT state (${}^1(\text{A}^{\bullet-}-\text{D}^{\bullet+})^*$)¹⁵ can be formed by charge recombination between $\text{REPy}^{\bullet+}$ and $\text{REPy}^{\bullet-}$ as shown in Scheme 3. Therefore, it is suggested that charge recombination between $\text{REPy}^{\bullet+}$ and $\text{REPy}^{\bullet-}$ with localized charges occurs to give ${}^1\text{REPy}^*$ with ICT character and ${}^1(\text{REPy})_2^*$ (for OPEPy and QEPy) and emit light during the pulse radiolysis of donor-acceptor-type REPy's in Bz. P-type

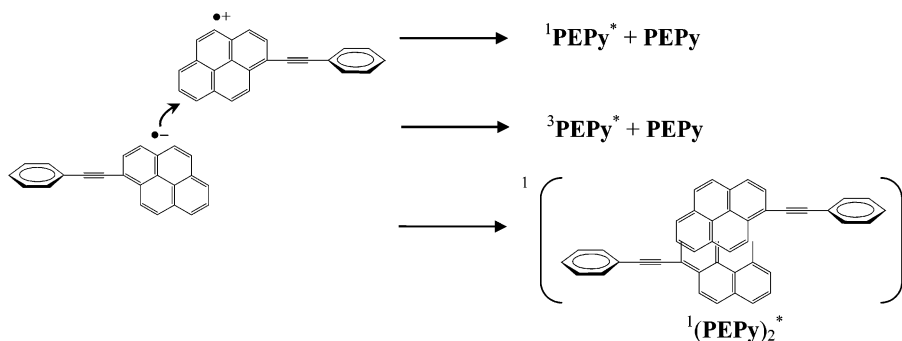
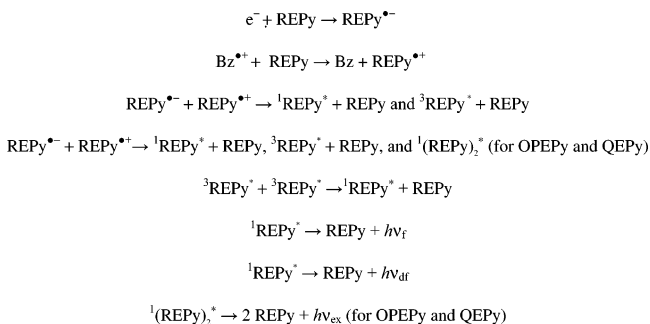
SCHEME 1: Proposed Structure for the Formation of PEPy in the S_1 and T_1 States (${}^1\text{PEPy}^*$ and ${}^3\text{PEPy}^*$, Respectively) and the Singlet Excimer (${}^1(\text{PEPy})_2^*$) during the Pulse Radiolysis of PEPy in Bz.

TABLE 6: Oxidation Potentials (E_{ox}) of the Donor Moieties, Reduction Potentials (E_{red}) of the Acceptor Moieties, and Estimated Annihilation Enthalpy Values ($-\Delta H^{\circ}$) and E'_{S_1} of Donor–Acceptor-Type REPy's in Bz

REPy	in CH ₃ CN		in CH ₃ CN		in Bz	
	donor	E_{ox}^a (V)	acceptor	E_{red}^a (V)	$-\Delta H^{\circ}$ (eV)	E'_{S_1} (eV)
NPEPy	<i>N,N</i> -dimethyl-aniline Py	0.55 ^b	Py	-2.38 ^c	3.22	2.59
OPEPy	isopropoxy-benzene		Py	-2.38		2.67
QEPy	Py	1.07 ^c	quinoline	-2.40 ^d	3.76	2.76
AEPy	Py	1.07	9-cyanoanthracene	-0.98 ^e	2.34	2.34

^a Potential was estimated versus Ag/Ag⁺. ^b Reference 14a. ^c Reference 9. ^d Reference 14b. ^e Reference 14c.

SCHEME 2: Plausible Mechanism of the Formation of the ICT Excited State ($^1(\text{A}^{\bullet-}-\text{D}^{\bullet+})^*$) during the Pulse Radiolysis of R_DEPy (NPEPy and OPEPy) and R_AEPy (QEPy and AEPy) in Bz.



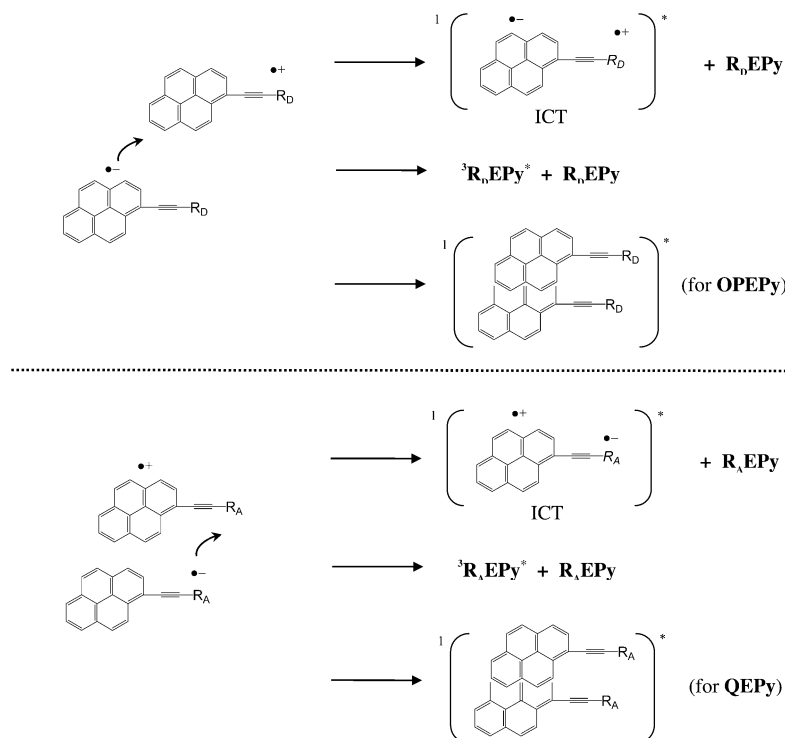
delayed fluorescence derived from the T-route was also observed for all REPy's in Bz during pulse radiolysis (Scheme 2).

The excimer emission peaks were observed at 510, 508, and 523 nm during the pulse radiolysis of PEPy, OPEPy, and QEPy, respectively. It is suggested that the ratio between the monomer and the excimer integrated areas should depend on geometries of the compounds and that a planar compound would be favorable for the excimer formation.⁷ It has been reported that

the DFT calculation indicated that NPEPy, AEPy, and PEPy have twisted geometries and that OPEPy and QEPy have planar geometries. The calculated dipole moments of the REPy's were 0.23, 1.01, 2.23, 3.28, and 5.98 D for PEPy, QEPy, OPEPy, NPEPy, and AEPy, respectively.⁵ It is suggested that for OPEPy and QEPy both π -stacking interactions between two Py's and between two isopropoxyphenyl or quinoline moieties are responsible for the formation of an encounter complex of REPy's with a proximally parallel geometry under the charge recombination between REPy^{•+} and REPy^{•-} to give the excimer emission (Scheme 3). For PEPy, it is suggested that PEPy^{•+} and PEPy^{•-} collide neck-to-neck to generate the excimer in which two Py moieties are stacked in the face-to-face structure with the benzene rings projecting perpendicularly away from each other due to the twisted geometry (Scheme 1). For NPEPy and AEPy, considerably twisted structures due to the strong electron donating or withdrawing substituents reduce the π -stacking interaction.

In addition, it should be noted that the excimer emission peaks of OPEPy (508 nm) and QEPy (523 nm) were observed at slightly shorter and longer wavelengths, respectively, than that of PEPy (510 nm). Both the HOMO and the LUMO of PEPy are mainly localized on the ethynyl-substituted Py moiety.

SCHEME 3: Mechanism of the Emission during the Pulse Radiolysis of Donor–Acceptor-Type REPy's in Bz.^a



^a REPy's are represented as (A–D) in which A and D denote R and/or Py moieties, respectively. $h\nu_{\text{f}}$, $h\nu_{\text{ex}}$, and $h\nu_{\text{df}}$ denote fluorescence from the monomer, from the excimer, and P-type delayed emission derived from triplet–triplet annihilation, respectively. REPy^{•-} = A^{•-}–D, REPy^{•+} = A–D^{•+}, ${}^1\text{REPy}^* = {}^1(\text{A}^{\bullet-}-\text{D}^{\bullet+})^*$.

However, the HOMOs of OPEPy and QEPy are localized on the isopropoxyphenyl group and the ethynyl-substituted Py moiety, respectively, while the LUMOs of OPEPy and QEPy are localized on the ethynyl-substituted Py moiety and quinoline moiety, respectively. The excimer emission peak of OPEPy was observed at a shorter wavelength than that of PEPy because of the stabilization of the HOMO by the substituents, while the LUMO is unaffected by the substituents. The excimer emission peak of QEPy was observed at a longer wavelength than that of PEPy because of the stabilization of the LUMO by the substituents, while the HOMO is unaffected by the substituents. It is found that the emission mechanism in pulse radiolysis strongly reflects on the localized MOs (HOMO and LUMO) of REPy's in the ground state, and the charge localization in REPy^{•+} and REPy^{•-} resulted from the presence of electron donating or withdrawing substituents connected through the ethynyl linkage.

Conclusions

Several substituted REPy's with or without donor–acceptor character showed efficient monomer and excimer emissions during pulse radiolysis in Bz. On the basis of the transient absorption and emission measurements and steady-state measurements, the emission is suggested to originate from ¹REPy*, which is generated from the charge recombination between REPy^{•+} and REPy^{•-} which are yielded from the initial radiolytic reaction in Bz. From DFT calculations, the calculated HOMO and LUMO surfaces of the REPy's are assumed to be localized. Thus, it is suggested that for PEPy the one-electron oxidation and reduction occur in the Py moieties of PEPy^{•+} and PEPy^{•-}, respectively. For donor–acceptor-type REPy's, the one-electron oxidation and reduction occur from the donor and acceptor moieties, respectively. This scheme reasonably explains why the $-\Delta H^\circ$ values (2.34–3.76 eV) estimated for the charge recombination between REPy^{•+} and REPy^{•-} are sufficiently larger than the emission maximal energies (E'_{s_i}) of the REPy's (2.34–2.93 eV). OPEPy and QEPy with planar structures showed the usual π -stacked excimer emission, while twisted PEPy exhibited the excimer in which two Py moieties are stacked in the face-to-face structure with the benzene rings projecting perpendicularly away from each other. These emission mechanisms in pulse radiolysis are considered to depend strongly on the charge localization of REPy^{•+} and REPy^{•-}, which can be achieved in the presence of electron donating or withdrawing substituents connected through an ethynyl linkage. It is emphasized that all REPy's show emissions during pulse radiolysis in benzene, while only two compounds (NPEPy and OPEPy) emit ECL. The large different results were compared, and the different reaction mechanisms were discussed.

Acknowledgment. We thank the members of the Radiation Laboratory of the Institute of Scientific and Industrial Research, Osaka University, for running the linear accelerator. This work

has been partly supported by a Grant-in-Aid for Scientific Research on Project 17105005 Priority Area 417, 21st Century COE Research, and others from the Ministry of Education, Culture, Sports, Science and Technology of the Japanese Government.

Supporting Information Available: Transient absorption spectra observed during the laser flash photolysis of the REPy's (20–80 μ M) in Ar-saturated Bz. This material is available free of charge via the Internet at <http://pubs.acs.org>.

References and Notes

- (1) (a) Fox, M. A.; Chanon, M. *Photoinduced Electron Transfer*; Elsevier: Amsterdam, 1988. (b) Kavarnos, G. J.; Turro, N. J. *Chem. Rev.* **1986**, *86*, 401.
- (2) (a) Faulkner, L. R.; Bard, A. J. *Electroanalytical Chemistry*; Marcel Dekker: New York, 1977; Vol. 10, pp 1–95. (b) Bard, A. J.; Faulkner, L. R. *Electrochemical Methods Fundamentals and Applications*, 2nd ed.; John Wiley and Sons: New York, 2001, pp 736–745. (c) Richter, M. M. *Chem. Rev.* **2004**, *104*, 3003.
- (3) (a) Samori, S.; Hara, M.; Tojo, S.; Fujitsuka, M.; Yang, S.-W.; Elangovan, A.; Ho, T.-I.; Majima, T. *J. Phys. Chem. B.* **2005**, *109*, 11735. (b) Samori, S.; Tojo, S.; Fujitsuka, M.; Yang, S.-W.; Elangovan, A.; Ho, T.-I.; Majima, T. *J. Org. Chem.* **2005**, *70*, 6661.
- (4) (a) Elangovan, A.; Chen, T.-Y.; Chen, C.-Y.; Ho, T.-I. *Chem. Commun.* **2003**, 2146. (b) Elangovan, A.; Yang, S.-W.; Lin, J.-H.; Kao, K.-M.; Ho, T.-I. *Org. Biomol. Chem.* **2004**, *2*, 1597. (c) Elangovan, A.; Chiu, H.-H.; Yang, S.-W.; Ho, T.-I. *Org. Biomol. Chem.* **2004**, *2*, 3113. (d) Elangovan, A.; Kao, K.-M.; Yang, S.-W.; Chen, Y.-L.; Ho, T.-I.; Su, Y. O. *J. Org. Chem.* **2005**, *70*, 4460.
- (5) Yang, S.-W.; Elangovan, A.; Hwang, K.-C.; Ho, T.-I. *J. Phys. Chem. B.* **2005**, *109*, 16628.
- (6) Kiyooki, H.; William R. W. *Chem. Phys.* **1980**, *51*, 61.
- (7) Lai, R. Y.; Fleming, J. J.; Merner, B. L.; Vermeij, R. J.; Bodwell, G. J.; Bard, A. J. *J. Phys. Chem. A.* **2004**, *108*, 376.
- (8) Gross, E. M.; Anderson, J. D.; Slaterbeck, A. F.; Thayumanavan, S.; Barlow, S.; Zhang, Y.; Marder, S. R.; Hall, H. K.; Nabor, M. F.; Wang, J.-F.; Mash, E. A.; Armstrong, N. R.; Wightman, R. M. *J. Am. Chem. Soc.* **2000**, *122*, 4972.
- (9) Santa Cruz, T. D.; Akins, D. L.; Birke, R. L. *J. Am. Chem. Soc.* **1976**, *98*, 1677.
- (10) (a) Liu, D. K. K.; Faulkner, L. R. *J. Am. Chem. Soc.* **1977**, *99*, 4594. (b) Bohne, C.; Abuin, E. B.; Scaiano, J. C. *J. Am. Chem. Soc.* **1990**, *112*, 4226.
- (11) (a) Shida, T.; Hamill, W. H. *J. Chem. Phys.* **1966**, *44*, 2369. (b) Shida, T.; Kato, T. *Chem. Phys. Lett.* **1979**, *68*, 106. (c) Grimison, A.; Simpson, G. A. *J. Phys. Chem.* **1968**, *72*, 1776. (d) Ishida, A.; Fukui, M.; Ogawa, H.; Tojo, S.; Majima, T.; Takamuku, S. *J. Phys. Chem.* **1995**, *99*, 10808. (e) Majima, T.; Tojo, S.; Ishida, A.; Takamuku, S. *J. Org. Chem.* **1996**, *61*, 7793. (f) Majima, T.; Tojo, S.; Ishida, A.; Takamuku, S. *J. Phys. Chem.* **1996**, *100*, 13615.
- (12) (a) Honda, E.; Tokuda, M.; Yoshida, H.; Ogasawara, M. *Bull. Chem. Soc. Jpn.* **1987**, *60*, 851. (b) Huddleston, R. K.; Miller, J. R. *J. Phys. Chem.* **1982**, *86*, 2410. (c) Majima, T.; Fukui, M.; Ishida, A.; Takamuku, S. *J. Phys. Chem.* **1996**, *100*, 8913. (d) Majima T.; Tojo, S.; Takamuku, S. *J. Phys. Chem. A* **1997**, *101*, 1048.
- (13) Shida, T. *Electronic Absorption Spectra of Radical Ions*; Elsevier: Amsterdam, 1988.
- (14) (a) Totah, R. A.; Hanzlik, R. P. *Biochemistry* **2004**, *43*, 7907. (b) Millefiori, S. *J. Heterocycl. Chem.* **1970**, *7*, 145. (c) Lewis, F. D.; Bedell, A. M.; Dykstra, R. E.; Elbert, J. E.; Gould, I. R.; Farid S. *J. Am. Chem. Soc.* **1990**, *112*, 8055.
- (15) Kawai, M.; Itaya, K.; Toshiba, S. *J. Phys. Chem.* **1980**, *84*, 2368.